

LASER SHOCK COMPRESSION AND SPALLING OF REACTIVE NI-AL LAMINATE COMPOSITES

C. T. Wei¹, B. R. Maddox², T. P. Weihs³, A. K. Stover³, V. F. Nesterenko¹, and M. A. Meyers¹

¹University of California, San Diego, La Jolla, CA-92093-0411

²Lawrence Livermore National Laboratory, Livermore, CA-94551

³Johns Hopkins University, Baltimore, MD-21218

Abstract. Reactive laminates produced by successive rolling and consisting of alternate layers of Ni and Al (with bi-layer thicknesses of 5 and 30 μm) were investigated by subjecting them to laser shock-wave loading. The laser intensity was varied between $\sim 2.68 \times 10^{11} \text{W/cm}^2$ (providing an initial estimated pressure $P \sim 25 \text{ GPa}$) and $\sim 1.28 \times 10^{13} \text{W/cm}^2$ ($P \sim 333 \text{ GPa}$) with two distinct initial pulse durations: 3 ns and 8 ns. Hydrodynamic calculations (using commercial code HYADES) were conducted to simulate the behavior of shock-wave propagation in the laminate structures. SEM, and XRD were carried out on the samples to study the reaction initiation, and the intermetallic compounds. It was found that the thinner bilayer thickness (5 μm) laminate exhibited the most intensive localized interfacial reaction at the higher laser intensity ($1.28 \times 10^{13} \text{W/cm}^2$); the reaction products were identified as NiAl and other Al-rich intermetallic compounds. The reaction front and the formation of intermetallic compounds extend into the sample with a thinner bilayer thickness (5 μm) to a depth of about 50 μm . Increase in the duration of laser shock wave induces increased reaction, which occurs also in the thicker bilayer laminate samples (30 μm bi-layer thickness). It is demonstrated that the methodology of laser shock is well suited to investigate the threshold conditions for dynamic mechanical reaction initiation caused by high intensity laser.

Keywords: Laminates, Ni/Al, laser shock, reaction, intermetallic compounds.

PACS: 01.30.Cc, 62.50.-p, 62.50.Ef, 68.65.Ac.

INTRODUCTION

Reactions in Ni-Al binary system have been intensively investigated on laminates and powders. Intermetallic products of Ni/Al binary system are NiAl, NiAl₃, Ni₂Al₃, and Ni₃Al [1]. These intermetallic compounds have exothermic reactions and release energies varying from 37.6 kJ/mol \times atom to 64.6 kJ/mol \times atom (37.6 kJ/mol \times atom for NiAl₃, 58.6 kJ/mol \times atom for Ni₂Al₃, and 64.6 kJ/mol \times atom for NiAl) [2] and facilitate the self-propagating high temperature synthesis (SHS).

EXPERIMENTAL PROCEDURE

The laminates were made by cold-rolling of alternatively stacked Ni and Al sheets [3]. The reductions of thickness were $\sim 85\text{-}90\%$ after cold-rolling and the total thicknesses of the laminates were 0.8–0.9mm, with average bilayer thickness of 5 and 30 μm .

The morphologies of the cross sections for the two different bilayer thicknesses are shown in Fig. 1. The differences in the thicker bilayer sample with orientation due to the rolling process are shown in Fig. 1 (a) and (b). The transverse section shows distinct shear bands running at an angle to

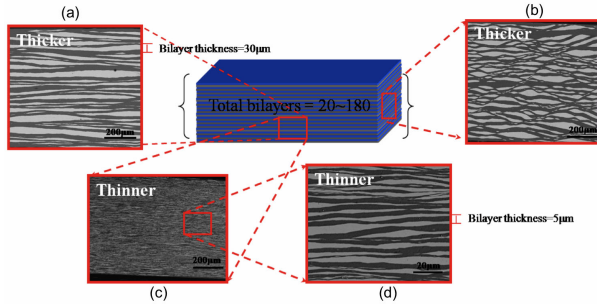


Figure 1. Cross sections of laminates: (a) Laminates of thicker (30µm) bilayer (Ni+Al), longitudinal section (b) Transverse section (c) Laminates with thinner (5µm) bilayer. (d) High magnification of thinner bilayer the Ni and Al layers. These bands are due to shear localization, a common occurrence in high strain deformation in rolling. The microstructural features along the longitudinal and transverse sections of the thinner sample (5 µm) bilayer laminate are identical (Fig. 1(c) and (d)).

The Jupiter laser facility of Lawrence Livermore National Laboratory was used for the experiments. The wavelength of laser is 532 nm. The laser energies were varied from ~24 to ~440J with durations of 3ns and 8ns and a square beam size, 1.12 mm². A phase-plate was used to distribute the laser energy homogeneously over the area of exposure.

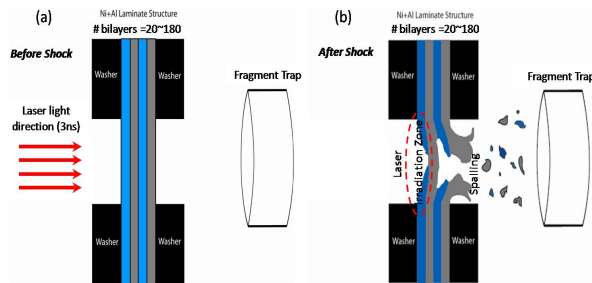


Figure 2. Schematic of laser shock: (a) Sample placed between laser irradiation source and fragment trap. Washers were used to fix samples. (b) Damage after laser irradiation

The front surface shows a crater (Fig. 2 (a)) and the back surface (Fig. 2 (b)) spalls after the shock pulse reflects from this surface. Fragments were captured by a fragment trap. A Rigaku MiniFlex II unit was used for x-ray diffraction (XRD). A Philips XL30 ESEM (BSE images) unit was used to investigate the recovered samples.

RESULTS AND DISCUSSION

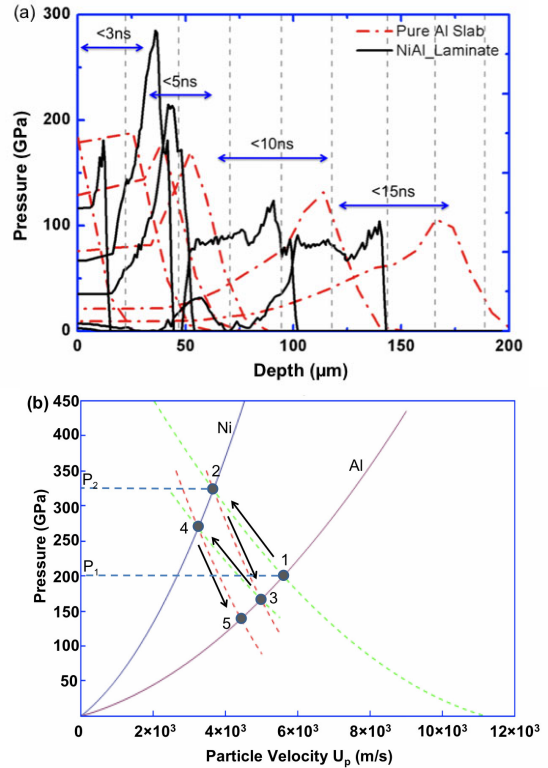


Figure 3. (a) Laser shock wave (400J 3ns) propagation in pure Al slab (dashed line) and laminate (full line) (HYADES Simulation) (b) Rankine-Hugoniot pressure vs. particle velocity plot for Ni and Al showing wave reflections.

The hydrodynamic code HYADES was used for characterization of laser propagation. Fig 3 (a) shows the 400J 3ns laser pulse propagation through Ni-Al laminate, as compared to monolithic Al. The computation reveals that a higher pressure was experienced when the shock wave reaches a surface of Ni layer after passing through an Al layer.

This impedance mismatch may cause the interfacial region of the nickel and the aluminum sheets to become more reactive. In comparison, no such phenomena were found in a pure Al slab and a monotonic decay is observed (Fig. 3(a), dash curves). This shock impedance phenomenon can be visualized by means of Fig. 3 (b). The interfacial pressures can be estimated as the waves reflect in the pressure-particle velocity plot (Fig. 3 (b)),

following the sequence $1 \rightarrow 2 \rightarrow 3 \rightarrow 4 \rightarrow 5$. This reverberation sequence shows that, as the shock front exits an Al layer and enters a Ni layer, the pressure increases; the reverse occurs when the shock front enters an Al layer coming from a Ni layer.

Lindl's equation [5] was also used to estimate the initial pressures (P).

$$P = 4 \times 10^3 \left(\frac{I_{15}}{\lambda} \right)^{\frac{2}{3}}$$

The I_{15} is the laser intensity (in 10^{15} W/cm²), and λ is the wavelength (532×10^{-3} μm). The initial pressures for different laser conditions are given in Table 1. The initial pressures are strongly related to the pulse duration.

Table 1. Initial Pressures (From Lindl's equation)

Sample	8ns pressure (GPa)	Intensity (8ns) (W/cm ²)	3ns pressure (GPa)	Intensity (3ns) (W/cm ²)
5 μm	114	2.56×10^{12}	131	3.18×10^{12}
			333	1.28×10^{13}
30 μm	25	2.68×10^{11}	130	3.13×10^{12}
	167	4.56×10^{12}	328	1.25×10^{13}

Fig 4 (a) shows that the thinner bilayer sample at 400J laser energy (3ns) has intensive reaction. The reactions propagate into the sample to a depth of about 50 μm. The arrow represents the incident direction of laser. The cross-sectional image at the edge of crater (Fig. 4 (b)) suggests that reaction did not propagate out of the crater area. No reaction was found on thicker bilayer experiments with 3ns laser pulse duration. Increasing the pulse duration (8ns) facilitates the thicker bilayer sample to overcome the reaction barrier (Fig. 5 (a)); however the reaction is not obvious at the edge of the crater (Fig. 5 (b)), which is identical to Fig. 4 (b).

A mechanism of intermetallic compound formation in shock compression was proposed by Meyers, Vecchio, and Yu [6, 7]. The sequence of Fig. 6 shows the principal concept. The solid Al and Ni layers (Fig. 6(a)) represent the original state of the laminate. When laser energy is applied to the surface of laminates, the Al layer melts and initial intermetallic nucleation takes place at the interface of Ni/Al layers (Figs. 6 (b)). After reaction

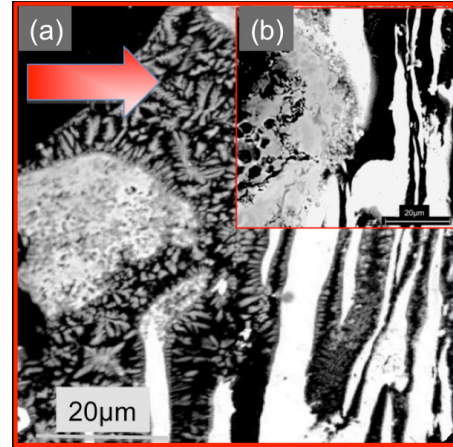


Figure 4. Cross-sectional observations (SEM-BSE) of 5 μm bilayer laminates: (a) 400J, 3ns laser (b) 400J, 3ns at the edge of crater

proceeds for a certain time, the intermetallic compounds agglomerate into spherules at the interface, and grow as elongated granules (Fig. 6 (c)), leading eventually to the formation of dendritic structures. As the granules and dendrites reach a critical size, the neighboring spheres start to grow and constrain the first spheres. The constraining effect expels the first granules and disperses them into the liquid Al layer (Fig. 6 (d)). The dispersed granules and dendrites may accumulate and cluster to become full dendrites due to the residual thermal energy (Fig. 4 (a)).

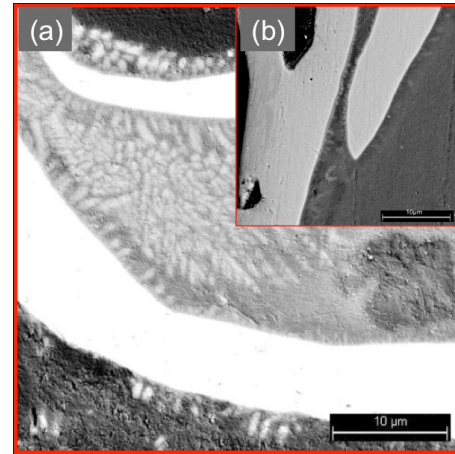


Figure 5. Cross-sectional observations (SEM-BSE) of 30 μm bilayer laminates: (a) 400J, 8ns laser (b) Reaction at the edge of crater.

X-ray diffraction analysis shows that the thicker bilayer sample has no intermetallic

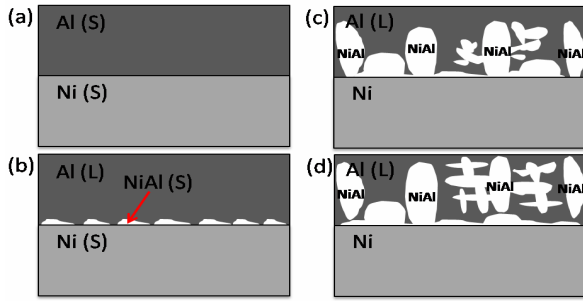


Figure 6. Sequence of reaction: (a) Original bilayer with solid Al and Ni layers; (b) Under laser shock, Al melts and interfacial reaction starts; (c) NiAl granules grow, become elongated, and start to form dendritic structures; (d) Dendrites and spherules are expelled due to the formation of new growing NiAl granules at the Ni-Al interface.

compound at 3ns laser shock (Fig.7 (a)), which is consistent with SEM. The dominant intermetallic compound is NiAl for 3ns laser pulse experiments. Longer pulse duration increases the reaction and helps to overcome the reaction barrier in thicker bilayer samples, which is shown in Fig. 7 (b). The intermetallic compounds NiAl and NiAl₃ were found for the 8ns pulse duration experiments.

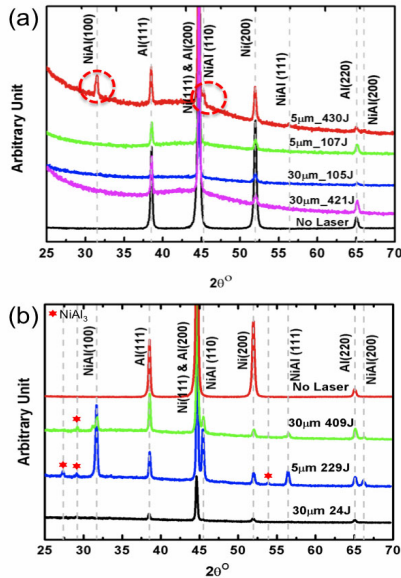


Figure 7. X-Ray diffraction of cross sectional surfaces of (a) 3ns and (b) 8ns laser pulse duration.

CONCLUSIONS

The following principal conclusions were reached:

1. The laser energy was insufficient to generate reaction propagation through the whole sample.
2. The bilayer thickness is an important geometrical factor for laser-induced reaction. Thinner Ni-Al bilayers (5µm) demonstrated sub-critical/critical behavior forming molten Al and Ni-Al compounds.

3. The reaction was confined to the laser irradiated area even at 400J irradiation energy and 8ns pulse duration.

4. Laser shock duration is an important factor to create reaction for both thinner and thicker bilayer samples under relatively lower laser intensity.

Acknowledgements: Funding was provided by Grant ONR MURI N00014-07-1-0740 and ILSA Contract No. W-7405-Eng-48. The help provided by Dr. D. Correll is gratefully acknowledged. The authors appreciate the generous help from Prof. Gustaf Arrhenius and Saul Perez-Montano for XRD analysis.

REFERENCES

1. Ansara I., Dupin N., Lukas H. L., Sundman B., "Thermodynamic Assessment of The Al-Ni System", *J. Alloys Comp.*, 247, 20, 1997.
2. Dong S., Hou P., Yang H., and Zou G., "Synthesis of Intermetallic NiAl by SHS Reaction Using Coarse-grained Nickel and Ultrafine-grained Aluminum Produced by Wire Electrical Explosion", *Intermetallics*, 10, 217, 2002.
3. Stover A. K., Walker N. K., Knepper R., Fritz G. M., Hufnagel T. C., and Weihs T. P., "Correlating Mechanical Properties to Microstructure in Rolled Nickel Aluminum Reactive Laminates", (Boston, JANNAF Conference, 2008).
4. Meyers M. A., "Dynamic Behavior of Materials", (John Wiley & Sons, Inc., 1994).
5. Lindl J., "Development of The Indirect-drive Approach to Inertial Confinement Fusion and The Target Physics for Ignition and Gain", *Phys. Plasmas*, 2, 3933, 1995.
6. Meyers M. A., Yu L.-H., and Vecchio K. S., "Shock Synthesis of Silicides-II. Thermodynamics and Kinetics", *Acta Metall. Mater.*, 42, 715, 1994.
7. K. S. Vecchio, L.-H. Yu, and M. A. Meyers, "Shock Synthesis of Silicides-I. Experimentation and Microstructural Evolution", *Acta Metall. Mater.*, 42, 701, 1994.